Available online at www.sciencedirect.com
SCIENCE DIRECT®
International Journal of Multiphase Flow 32 (2006) 82–105
International Journal of Multiphase Flow
www.elsevier.com/locate/ijmulflow

Closure relations for two-fluid models for two-phase stratified smooth and stratified wavy flows

A. Ullmann, N. Brauner *

Faculty of Engineering, Tel-Aviv University, Tel-Aviv 69978, Israel

Received 15 August 2004; received in revised form 25 August 2005

Abstract

The theory-based closure relations for the wall and interfacial shear stresses obtained previously for laminar stratified flow, are extended to be applicable also to turbulent flows in either or both of the phases. The closure relations are formulated in terms of the single-phase-based expressions, which are augmented by two-phase interaction factors, due to the flow of the two phases in the same channel. These closure relations, which are valid for smooth stratified flow in horizontal or inclined pipes, were used as a platform for introducing necessary empirical corrections required in the stratified wavy flow regime. Based on experimental data available from the literature, new empirical correlations for the wave effect on the interface curvature, on the interfacial shear and on the liquid wall shear were obtained. The predictions of the two-fluid model for the pressure gradient and holdup are tested against extensive data bank and some analytical solutions for stratified flows. The favorable comparison suggest that the new closure relations are essentially representing correctly the interaction between the phases over a wide range of flow parameters space in the stratified smooth and stratified wavy regimes. The difficulties encountered due the possibility of obtaining multiple solutions in inclined flows are discussed.

Keywords: Stratified flow; Two-fluid; Closure; Interfacial shear; Wall shear; Interface curvature; Turbulent

1. Introduction

Two-phase stratified flow is often observed in horizontal or slightly inclined systems in a gravity field. This flow pattern is encountered in petroleum transportation pipes, in the nuclear and process industries under steady or transient conditions.

The key engineering design parameters are the pressure drop and average in situ holdup and velocities. Their prediction is commonly attempted via the two-fluid (1-D) model. However, the application of two-fluid model is dependent on the presumed interface shape (either plane or curved) and on the availability of reliable closure relations for the wall shear and interfacial shear stresses (averaged over the corresponding wetted perimeter) in terms of the local/instantaneous holdup and velocities. These closure relations should correctly

* Corresponding author.
E-mail address: brauner@tau.eng.ac.il (N. Brauner).

0301-9322/$ - see front matter © 2005 Published by Elsevier Ltd.
doi:10.1016/j.ijmultiphaseflow.2005.08.005

represent the effects of the systems parameters (e.g. fluids' flow rates and physical properties, tube diameter and inclination) and the flow regime in either of the phases (laminar or turbulent).

The stratified flow regime is divided into two main sub-regimes: the stratified smooth and the stratified wavy regimes. A smooth interface between the phases can be obtained only in a limited range of sufficiently low flow rates. With increasing the relative velocity between the two layers the interface become unstable. Typically, in gas–liquid systems, with increasing the gas flow rate at a constant liquid rate, small amplitude, regular waves first appear. The wave amplitude increases with the gas flow rate resulting in irregular, three-dimensional large amplitude roll waves, with possible drop entrainment from their crest. These interfacial waves increase drastically the drag between the phases, and consequently cause a considerable increase in the pressure gradient.

The modeling of the interfacial momentum transfer is considered the crucial issue in gas–liquid stratified flows. The approach that is commonly followed is to use closure relations that are based on the knowledge gained in single-phase flows, assuming these are valid for smooth stratified flow. Then, empirical corrections were introduced to match with two-phase flow data in the stratified wavy regime. For Example, in gas–liquid systems the interfacial shear stress is commonly modeled based on the flow of the gas phase. Then, either empirical correlations for the interfacial friction factor (e.g. Cohen and Hanratty, 1968; Kawaji et al., 1987; Kowalski, 1987), or empirical correction factors on the gas friction factor (e.g. Andritsos and Hanratty, 1987; Andreussi and Persen, 1987; Ottens et al., 1997, 1999), or correlations for the equivalent sand roughness (e.g. Hamersma and Hart, 1987; Oliemans, 1987) were obtained based on experimental data. However, the interfacial waves affect also the liquid wall shear stress, in particular in cases of thin liquid layers. Therefore, empirical correlations were derived also for the liquid wall friction factor (e.g. Kowalski, 1987; Hagiwara et al., 1989; Vlachos et al., 1997, 1999). Moreover, the shape of the interface in wavy flow is in fact unknown. While most of the empirical correlations developed for the interfacial and wall shear stresses assumed a time-averaged plane interface, experiments indicate that in the wavy regime the gas–liquid interface is concave. Therefore, on top of the three closure relations for the shear stresses, an additional closure relation is in fact required to determine the stratified flow geometry (Hamersma and Hart, 1987; Hart et al. (1989), Chen et al., 1997; Watterson et al., 2002). Obviously, these four closure relations are not independent. For a specified holdup (and pressure drop), the wetted perimeters are subject to variation upon changing the flow geometry. Consequently, different values for the wall and interfacial shear stresses are implied by the two-fluid momentum equations to match experimental data of the pressure drop and/or the holdup.

In a recent study (Ullmann et al., 2004) it was shown that there are some basic pitfalls in the commonly used single-phase-based closure relations for the two-fluid (TF) models. These cause the TF model predictions to fail even in the case the interface is smooth and plane and the flow in the two phases is laminar. Difficulties are encountered already when the TF is applied to horizontal systems. These become more pronounced in the case of inclined systems, where the holdup and pressure drop result from a fine balance between shear and gravity forces. The pitfalls of the single-phase-based closure relations were rigorously identified in that study in view of corresponding results obtained via the exact solution for fully developed stratified laminar pipe flow (LPF).

New, theory-based closure relations for laminar stratified flow were derived in Ullmann et al. (2004) for the wall and interfacial shear stresses, which account for the interaction between the phases. The new closure relations were formulated in terms of the single-phase-based expressions, which are augmented by the two-phase interaction factors. The TF model predictions obtained with these new closure relations (denoted as MTF model) were tested against the LPF exact solution. Very good results were obtained for the pressure drop and holdup for a wide range of dimensionless parameters in co-current and counter-current laminar stratified flows. However, although laminar stratified flow is frequently encountered in liquid–liquid systems, it may be of limited relevance to practical applications of gas–liquid flows.

The purpose of the present study is first to extend the MTF closure relations for the case of turbulent stratified flows with smooth and flat interface (Section 2). The MTF predictions are validated by comparison with the results obtained for the case of pseudo-single-phase turbulent pipe flow and with pressure drop and holdup data of Espedal (1998) for turbulent gas–liquid stratified flow with a smooth interface. These closure relations are then used as a platform for introducing necessary empirical corrections for the stratified wavy regime. In fact, the wave effect can be evaluated only with a reference to a model that uses reliable closure relations for

cases of smooth interface. Based on the experimental data of Ottens (1998) and Chen et al. (1997) for holdups and wall wetted perimeters in the stratified wavy regime, a new correlation is obtained for the curvature of the gas–liquid interface (Section 3.1). This correlation, combined with pressure drop and holdup data from the literature for co-current horizontal (Chen et al., 1997; Ottens, 1998; Badie et al., 2000) upward and downward inclined stratified flows (Ottens, 1998; Espedal, 1998), are used to obtain new empirical corrections for the wave effect on the interfacial shear stress and on the liquid wall shear stress (Section 3.2).

The results of this study indicate that the new closure relations are essentially representing correctly the interaction between the phases over a wide range of parameters in the stratified smooth and stratified wavy regime.

2. Smooth stratified flow

The stratified flow configuration and coordinates are schematically described in Fig. 1. The inclination angle, β is always taken as positive. In co-current flow, the superficial velocities of the phases (U_{1s}, U_{2s}) are both positive in case of downward flow and negative for the case of upward flow. Whereas in counter-current flow U_{2s} is negative (the light phase flows upward).

Assuming a fully developed stratified flow, the integral form of the momentum equations for the two fluids are

$$-A_1\frac{\mathrm{d}p}{\mathrm{d}z}+\tau_1 S_1-\tau_i S_i+\rho_1 A_1 g\sin\beta=0 \tag{1.1}$$

$$-A_2\frac{\mathrm{d}p}{\mathrm{d}z}+\tau_2 S_2+\tau_i S_i+\rho_2 A_2 g\sin\beta=0 \tag{1.2}$$

where $A_{1,2}$ and $S_{1,2}$ are the cross-sectional area and the wall perimeter of each of the fluids respectively and S_i is the interfacial perimeter. The in situ holdup of the lower phase is $\varepsilon=4A_1/\pi D^2$. Eliminating the pressure drop yields

$$\tau_1\frac{S_1}{A_1}-\tau_2\frac{S_2}{A_2}-\tau_i S_i\left(\frac{1}{A_1}+\frac{1}{A_2}\right)+(\rho_1-\rho_2)g\sin\beta=0 \tag{2}$$

2.1. Modified two-fluid (MTF) closure relations

The closure relations adopted for the wall and interfacial shear stresses are basically of the same structure of the modified two-fluid (MTF) closure relations derived in Ullmann et al. (2004) for stratified laminar flows. Based on the exact solutions obtained for fully developed stratified laminar flow, it was shown that the single-phase-based closure relations for the shear stressed must be augmented by appropriate correction factors, which account for the interaction between the phases. The MTF closure relations are herein generalized to make them applicable also for cases of turbulent flow in either or both of the phases.

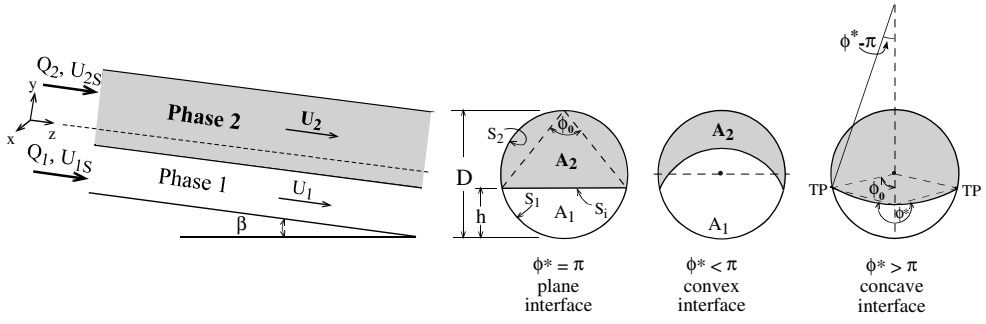

Fig. 1. Schematic description of the stratified flow configuration and coordinates.

The generalized expressions used for the wall shear stresses are

$$\tau_1 = -\frac{1}{2}\rho_1 f_1 |U_1| U_1 |F_1|^{n_1} \mathrm{sign}(F_1); \qquad U_1 = \frac{U_{1s}}{\varepsilon} \tag{3}$$

$$\tau_2 = -\frac{1}{2}\rho_2 f_2 |U_2| U_2 |F_2|^{n_2} \mathrm{sign}(F_2); \qquad U_2 = \frac{U_{2s}}{1-\varepsilon} \tag{4}$$

The friction factors f_1 and f_2 are based on the Reynolds number of the corresponding layer, each flowing as a single phase in its own channel. In case of hydrodynamic-smooth wall surface, the Blasius-type power-law expressions for the wall shear stresses can be used

$$f_1 = \frac{c_1}{Re_1^{n_1}}; \qquad f_2 = \frac{c_2}{Re_2^{n_2}} \tag{5.1}$$

with

$$Re_1 = \frac{\rho_1 |U_1| D_1}{\mu_1}; \qquad D_1 = \frac{4A_1}{(S_1 + S_i)} \tag{5.2}$$

$$Re_2 = \frac{\rho_2 |U_2| D_2}{\mu_2}; \qquad D_2 = \frac{4A_2}{(S_2 + S_i)} \tag{5.3}$$

Given the flow regime in the two phases the constants ($c_{1,2}$ and $n_{1,2}$ are prescribed, e.g. laminar: $c = 16$, $n = 1$, turbulent: $c = 0.046$, $n = 0.2$) the single-phase-based friction factors f_1, f_2 can be calculated. The factors F_1 and F_2 represent corrections of the single-phase-based expressions for the wall shear stresses due the interaction between the two fluids flowing in the same channel. It is worth emphasizing that the conventional TF closure relations assume $F_1, F_2 \equiv 1$. However, the hydraulic diameters D_1, D_2, (used to evaluate Re_1 and Re_2) are adjusted according to the relative velocity of the two phases; the interface is generally considered as 'stationary' (wetted) with respect to the flow of the faster phase and as 'free' with respect to the flow of the slower phase (Brauner and Moalem Maron, 1989). In the MTF closure relations, the hydraulic diameters D_1, D_2, (Eqs. (5.2) and (5.3)) are calculated by considering the fluids interface as 'stationary', for both phases regardless their relative velocity. The effects of variations of the effective hydraulic diameters due to the interaction between the phases are embodied in the F_1 and F_2 factors. These are given by

$$F_1 = \frac{1 + \dfrac{U_2}{U_1}\left[g_{11} X^2 \left(\dfrac{1-\varepsilon}{\varepsilon}\right)^2 - (2\varepsilon)^{1-n_2} g_{12}\right]}{1 + \dfrac{U_2}{U_1} X^2 \left(\dfrac{1-\varepsilon}{\varepsilon}\right)^2} \tag{6.1}$$

$$F_2 = \frac{1 + \dfrac{U_1}{U_2}\left[g_{22} \dfrac{1}{X^2}\left(\dfrac{\varepsilon}{1-\varepsilon}\right)^2 - (2(1-\varepsilon))^{1-n_1} g_{21}\right]}{1 + \dfrac{U_1}{U_2}\dfrac{1}{X^2}\left(\dfrac{\varepsilon}{1-\varepsilon}\right)^2} \tag{6.2}$$

The X^2 is the Martinelli parameter, representing the ratio between the superficial frictional pressure drops obtained in single phase flow of either of the phases. In terms of the superficial Reynolds number of the two phases (Re_{1s}, Re_{2s}) and the power-law exponents $n_{1,2}$ it is given by

$$X^2 = \frac{(-\mathrm{d}p_f/\mathrm{d}z)_{1s}}{(-\mathrm{d}p_f/\mathrm{d}z)_{2s}} = \frac{c_1}{c_2}\frac{Re_{1s}^{-n_1}}{Re_{2s}^{-n_2}}\frac{\rho_1}{\rho_2}|q|q; \qquad q = \frac{Q_1}{Q_2} = \frac{U_{1s}}{U_{2s}} \tag{6.3}$$

The g_{11}, g_{12}, g_{21}, g_{22} in Eqs. (6) are functions of the dimensionless wetted perimeters $\tilde{S}_1, \tilde{S}_2$ and $\tilde{S}_i$ in the pipe geometry, ($\tilde{S} = S/D$):

$$g_{11} = \frac{\tilde{S}_1}{\tilde{S}_1 + \tilde{S}_i}; \qquad g_{22} = \frac{\tilde{S}_2}{\tilde{S}_2 + \tilde{S}_i} \tag{7.1}$$

$$g_{12} = \frac{4}{\pi + 2}\frac{\tilde{S}_2}{\tilde{S}_2 + \tilde{S}_1}; \qquad g_{21} = \frac{4}{\pi + 2}\frac{\tilde{S}_1}{\tilde{S}_2 + \tilde{S}_1} \tag{7.2}$$

These functions were determined in Ullmann et al. (2004) based on the closure relations expected for τ_1 and τ_2 in stratified laminar flows.

Eqs. (3) and (4) indicate that for $F_1 = 1$ (or $F_2 = 1$), the wall shear stress corresponds to that obtained in single-phase flow of the lower (or upper) fluid in its own channel. Indeed, as $U_1/U_2 \to 0$, Eq. (6.2) yields $F_2 \to 1$. In this case the interface can be considered "stationary" with respect to the upper phase and the wall shear stress can be modeled based on single-phase correlations for the friction factor. This is a typical case in gas–liquid horizontal and upward inclined systems, where the gas velocity is usually much higher than the liquid velocity. In such cases of $U_2/U_1 \equiv U_G/U_L \gg 1$, and when also $X^2(1-\varepsilon)^2/\varepsilon^2 \gg 1$, Eq. (6.1) renders $F_1 \to g_{11} = S_1/(S_1 + S_i)$. As a result, $F_1^{n_1}$ modifies the hydraulic diameter D_1 (embedded in f_1) of the slower heavier phase to $4A_1/S_1$ (instead of $4A_1/(S_1 + S_i)$ as defined in Eq. (5.2)). This is equivalent to considering the interface as 'free' for the calculation of D_1, as commonly assumed in cases of $U_2/U_1 \gg 1$. Obviously, similar arguments apply for the opposite case of $U_2/U_1 \ll 1$, where the heavier fluid is the faster whereby $F_1 \to 1$ and $F_2 \to g_{22} = S_2/(S_2 + S_i)$. Evidently, the numerator of Eqs. (6) indicates that these F-interaction terms may attain negative values and thus, these closure relations are capable of representing the occurrence of reversed wall shear in cases of near-wall backflow in inclined flows (see Ullmann et al., 2004).

For the interfacial shear, the generalized MTF closure relations are

$$\tau_i = \begin{cases} -\frac{1}{2}\rho_1 f_{i1}|U_1|(c_{i2}U_2 - U_1)|F_{i1}|^{n_1}; & |F_{i1}|^{n_1} > |F_{i2}|^{n_2} \\ -\frac{1}{2}\rho_2 f_{i2}|U_2|(U_2 - c_{i1}U_1)|F_{i2}|^{n_2}; & |F_{i1}|^{n_1} \leqslant |F_{i2}|^{n_2} \end{cases} \tag{8.1}$$

with

$$F_{i1} = \frac{1}{1 + \frac{U_2}{U_1}X^2\left(\frac{1-\varepsilon}{\varepsilon}\right)^2}; \qquad F_{i2} = \frac{1}{1 + \frac{U_1}{U_2}\frac{1}{X^2}\left(\frac{\varepsilon}{1-\varepsilon}\right)^2}; \tag{8.2}$$

$$c_{i1} = \left|\frac{2q}{1+q}\right|^{1-n_2}; \qquad c_{i2} = \left|\frac{2}{1+q}\right|^{1-n_1} \tag{8.3}$$

For hydrodynamic-smooth pipe wall (and smooth interface)

$$f_{i1} = f_1; \qquad f_{i2} = f_2 \tag{8.4}$$

Note that the values of the coefficients c_{i1} and c_{i2} (Eqs. (8.3)) differ from one only in cases of turbulent flow, and generally their inclusion have only a mild effect on the pressure gradient and the holdup predictions. As their inclusion introduces a discontinuity in the TF model derivatives when switching between the two τ_i forms of Eq. (8.1), they can conveniently be omitted ($c_{i1}, c_{i2} = 1$).

The suggested structure of the closure relation for τ_i is different than that commonly used in TF models. Two-fluid models assume $F_i \equiv 1$, and τ_i is evaluated based on the wall shear stress of the faster phase, replacing its velocity head by the velocity difference $\tau_i \propto |U_2 - U_1|(U_2 - U_1)$. However, the MTF model suggests a different structure (see Ullmann et al., 2004); τ_i should be modeled based on a characteristic velocity difference times the faster fluid velocity. The same structure was found appropriate also to represent the interfacial shear in core annular flows (Ullmann and Brauner, 2004).

The F_{i1}, F_{i2} represent correction factors due to the interaction between the flows in the two layers. The first form in Eq. (8.1) corresponds to the case where the interfacial shear is dominated by the flow of the heavy phase, whereas the second form corresponds to a dominance by the light phase. Note that $0 < F_{i1,2} \leqslant 1$. The use of the first form, with F_{i1}, is convenient in case of a much faster heavier layer. In limiting cases of $\frac{U_2}{U_1}X^2\left(\frac{1-\varepsilon}{\varepsilon}\right)^2 \ll 1, F_{i1} \to 1$, the interfacial shear stress is in fact dominated by the flow of the lower-layer. On the other hand, in the opposite case of a much faster upper layer, $F_{i2} \to 1$, indicating that the interfacial shear stress is dominated by the flow of upper layer. The latter is the typical case in gas–liquid systems, where the interfacial friction factor is commonly assumed to be the same as the wall friction factor of the gas phase. However, the F_i interaction factors (Eq. (8.2)), and the criterion used in Eq. (8.1) for switching between the two alternative expressions for τ_i, suggest a matching between the solutions obtained with the two expressions

for the interfacial shear. The MTF closure relation for the interfacial shear thus minimises the discontinuity and other ill-effects encountered in the TF predictions (see Ullmann et al., 2003a).

For laminar stratified flow in both phases, $n_1 = n_2 = 1$, and $X^2 = \tilde{\mu}q$, where $\tilde{\mu} = \mu_1/\mu_2$. In this case the closure relations given in Eqs. (3)–(8) reduce to those presented in Ullmann et al. (2004). Note, however, that the Blasius power-law model for the wall friction factor (Eq. (5.1)) is valid for hydrodynamic smooth wall. In case of turbulent flow in a rough pipe, the wall friction factors are calculated by using Haland (1983) equation (see Appendix A). In fact, since the parameters of the power-law model for the friction factors ($c_{1,2}$, $n_{1,2}$) are Reynolds number dependent, the use of the logarithmic expressions for the friction factors is preferable also in cases of turbulent flow in smooth pipes (with zero roughness, $\kappa_s = 0$).

2.2. Interface shape

The interface shape is approximated by a constant curvature arc (Brauner et al., 1996; Gorelik and Brauner, 1999). Plane (flat) interface corresponds to $\phi^* = \pi$, concave interfaces are described by $\pi < \phi^* \leqslant 2\pi$, and convex interfaces by $0 < \phi^* \leqslant \pi$. The dimensionless geometrical variables in terms of ϕ_0 and ϕ^* are given in Table 1.

In gravity dominated systems and in the smooth stratified flow regime (no secondary flows), the interface is practically plane. Gravity dominated systems are associated with large Eotvos number ($Eo_D = \Delta\rho g D^2/8\sigma \gg 1$), corresponding to large diameter (D), high density difference ($\Delta\rho$) and low surface tension (σ) systems. The flow geometry can then be described either by the dimensionless wetted wall perimeter, ϕ_0 (see Table 1), or alternatively by the thickness of the (lower) fluid layer, $\tilde{h} = h/D = 0.5(1 - \cos\phi_0)$. However, if surface tension forces become important, the interface can be concave or convex, depending on the fluids/wall wetting angle, α and the holdup. A closure relation for the characteristic interface curvature of the form $\phi^* = \phi^*(Eo_D, \varepsilon, \alpha)$ was obtained by Brauner et al. (1996) and its incorporation with stratified flow models was studied in Brauner et al. (1998).

2.3. Solution procedure

The two-fluid momentum equations (Eqs. (1)), combined with the above closure relations for the shear stresses Eqs. (3)–(8) and for the interfacial curvature, comprise the generalized MTF model. Upon substituting the above closure relations in the combined momentum equation (2), an implicit equation for the interface location, ϕ_0 (or the holdup) is obtained. The dimensionless solution parameters are the Martinelli parameter, X^2, the flow rates ratio, q, the inclination parameter, $Y = [(\rho_1 - \rho_2)g\sin\beta]/(-\mathrm{d}p_f/\mathrm{d}z)_{2s}$ and the Eotvos number, Eo_D. Note, however, that in this study only gravity dominated systems will be considered, whereby in the smooth stratified flow regime the interface is plane. Co-current flows correspond to $X^2 > 0$ with $Y > 0$ (<0) for down-flow (up-flow). Counter-current flows correspond to $X^2 < 0$ and $Y < 0$.

Once a solution has been obtained for the in situ holdup, the corresponding pressure drop can be calculated by either of Eqs. (1) or from their sum. The total pressure drop is composed of the gravitational (hydrostatic) pressure drop, which is determined by the holdup:

$$\left(\frac{\mathrm{d}p_g}{\mathrm{d}z}\right) = [\rho_1\varepsilon + \rho_2(1-\varepsilon)]g\sin\beta = [\rho_2 + (\rho_1 - \rho_2)\varepsilon]g\sin\beta \tag{9}$$

Table 1
Flow geometry for plane and curved interfaces

	Curved interface, $\phi^* \neq \pi$	Plane interface, $\phi^* = \pi$
$\tilde{A} = A/D^2$	$\pi/4$	$\pi/4$
$\tilde{A}_2 = A_2/D^2$	$0.25\{\pi - \phi_0 + 0.5\sin(2\phi_0) - (\sin\phi_0/\sin\phi^*)^2[\pi - \phi^* + 0.5\sin(2\phi^*)]\}$	$0.25[\pi - \phi_0 + 0.5\sin(2\phi_0)]$
$\tilde{A}_1 = A_1/D^2$	$0.25\{\phi_0 - 0.5\sin(2\phi_0) - (\sin\phi_0/\sin\phi^*)^2[\phi^* - \pi - 0.5\sin(2\phi^*)]\}$	$0.25[\phi_0 - 0.5\sin(2\phi_0)]$
$\tilde{S}_2 = S_2/D$	$\pi - \phi_0$	$\pi - \phi_0$
$\tilde{S}_1 = S_1/D$	ϕ_0	ϕ_0
$\tilde{S}_i = S_i/D$	$(\pi - \phi^*)\sin(\phi_0)/\sin(\phi^*)$	$\sin(\phi_0)$

and the frictional pressure gradient $(-\mathrm{d}p_f/\mathrm{d}z)$. The dimensionless frictional pressure gradient is Π_f and the dimensionless difference in the hydrostatic pressure gradient, Π_g (compared to single phase flow of the light phase) are given by

$$\Pi_f = -\frac{\mathrm{d}p/\mathrm{d}z - (\mathrm{d}p_g/\mathrm{d}z)}{(-\mathrm{d}p_f/\mathrm{d}z)_{2s}}; \qquad \Pi_g = \frac{(\mathrm{d}p_g/\mathrm{d}z) - (\mathrm{d}p_g/\mathrm{d}z)_{2s}}{(-\mathrm{d}p_f/\mathrm{d}z)_{2s}} = Y\varepsilon \tag{10}$$

2.4. Validation of the MTF model—discussion

The effect of the flow regime on the MTF model predictions are demonstrated in Fig. 2 for a test case of air–water flow in an inclined pipe assuming the interface is plane and smooth. The significance of these assumptions is studied in the following Section 3 in view of the wave effects on the interface shape and shear stresses.

The constant inclination parameter used in Fig. 2 corresponds to a constant upward flow rate of air. In case of turbulent air flow, the value of the inclination parameter used ($Y = -15.5$) corresponds to $U_{2s} = U_{Gs} = 8.975$ m/s in a 2° upward inclined pipe ($D = 0.051$ m). A variation of the water flow rate is indicated in the figures by variation of X^2. The solution obtained with turbulent flow also in the liquid phase is indicated by T_L–T_G. The solution that assumes laminar flow of the liquid phase is denoted in the figure as L_L–T_G. However, its relevance is limited to the region of very low X^2($-0.01 < X^2 < 0.01$, $-0.002 < q < 0.002$), corresponding to low liquid flow rates.

The solution obtained with laminar flow in both phases (L_L–L_G) for the same value of the inclination parameter ($Y = -15.5$) corresponds to lower gas flow rates and a shallower inclination. The case of laminar flow in both phases is compared in Fig. 2 with the exact solution of the Navier–Stokes equations for fully-developed stratified laminar pipe flow (LPF solution, Ullmann et al., 2004). As shown, the MTF model predictions for the holdup (Fig. 2a) and for the frictional pressure gradient (Fig. 2b) in the case of laminar flow (L_L–L_G) are close to the values obtained by the LPF solution in the counter-current and co-current regions.

In the counter-current region, for each specified flow rate of the liquid phase, there are two solutions for the holdup (and pressure drop) up to the flooding point, beyond which no solution is obtained. One solution is of a relatively low holdup of the heavy phase, the other with high holdup of the heavy phase, which is the relevant mode when the resistance on the heavy-phase (liquid) outlet is increased. In liquid–liquid counter-current flow, both of these stratified flow modes were obtained experimentally (Ullmann et al., 2003a). In gas–liquid counter-current flow, the high liquid holdup mode is most probably unstable, due to wave bridging phenomena, resulting in transition to bubbly or plug flow.

As shown in Fig. 2, the solution of high liquid holdup is obtained also for all liquid upward flow rates in the co-current region. Stratified flow with high liquid holdup is generally not observed as it leads to slug formation. However, at the vicinity of positive $X^2 \approx 0$ (corresponding to low upward liquid flow rates), multiple (3) solutions are obtained (see the enlargements of this region in Fig. 2c). The additional two solutions of low liquid holdup may correspond to a stable stratified configuration. In fact, the range of liquid flow rates where triple holdups are predicted corresponds to the operational conditions where stratified flow was observed in upward gas–liquid flows (Ullmann et al., 2003a). Note that the T_L–T_G solution shown in Fig. 2c is not valid in this range of low liquid flow rates, since the liquid Reynolds number corresponds to laminar flow. Generally, multiple solutions in the counter-current and co-current flows are a result of different possible configurations that satisfies the fine balance between the gravitational and frictional forces for the same operational conditions.

In co-current inclined flows backflow can be encountered near the pipe walls. In upward co-current flow, downward backflow of the heavy phase can be obtained near the lower pipe wall. Similarly, in co-current down-flow, upward backflow of the light phase may result adjacent to the upper wall. Since in the conventional TF closure relations F_1, $F_2 \equiv 1$, the wall shear stress is determined by the flow direction as indicated by the average phase velocity hence the direction of the wall shear stress is erroneous in cases of near wall backflow. These situations can be handled by the MTF model, as the sign of the F-interaction factors may attain negative values, and thus affect a change of the direction of the wall shear stress (see Ullmann et al., 2004). In the case study of Fig. 2, the high liquid holdup solution in the region of $0 < X^2 < 1.5$ corresponds to reversed liquid wall shear, $F_1 < 0$. Note that some anomalous behavior of T_L–T_G holdup and pressure

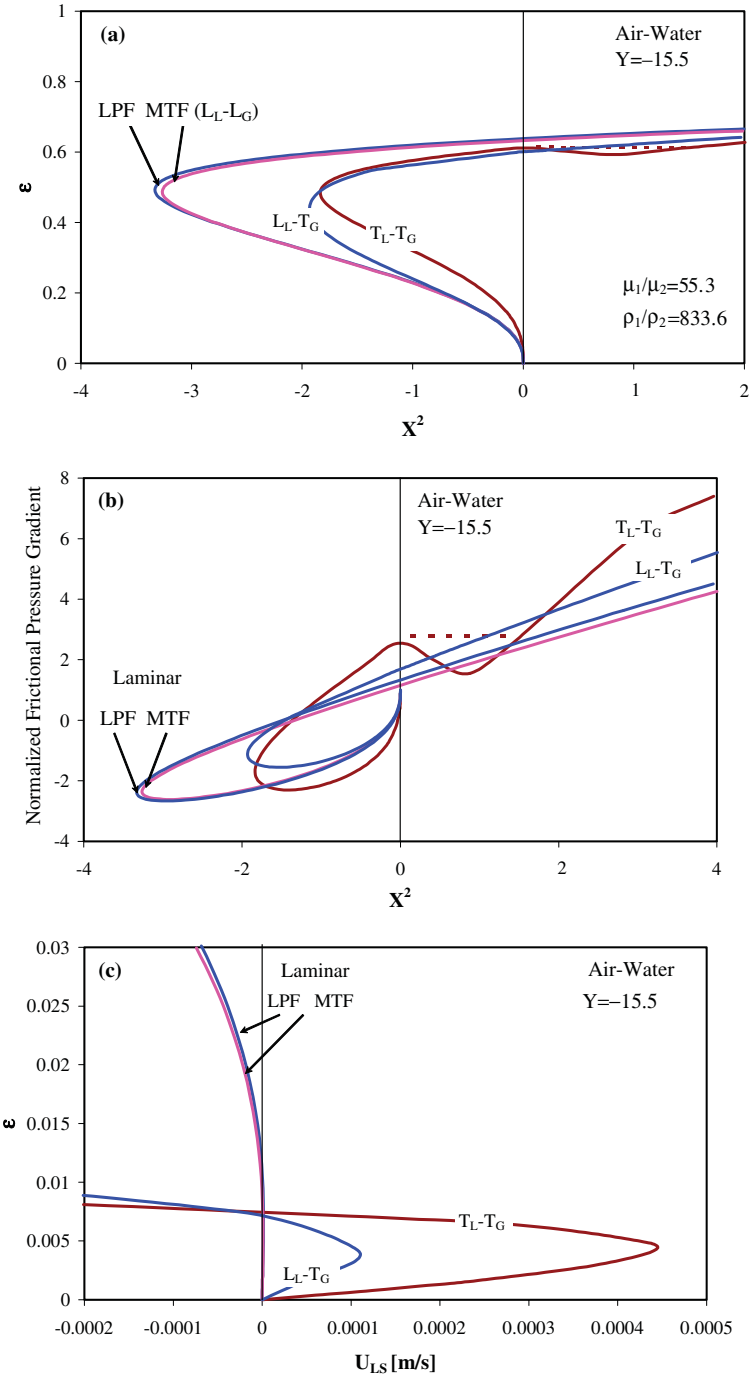

Fig. 2. The MTF model results for air–water laminar or turbulent smooth stratified flow, in a 2° inclined 0.051 m diameter pipe in the counter-current and co-current up-flow regions. Laminar flow are compared with the LPF exact solution (Ullmann et al., 2004): (a) holdup, (b) dimensionless frictional pressure gradient and (c) magnification of low liquid flow rates region.

gradient curves is obtained in the region where F_1 changes its sign. This anomaly is however smoothed out if small negative and positive F_1 values are replaced by $F_1 = 0$ (indicated by the dashed section in Fig. 2a).

In upward gas–liquid flow, however, the interface is wavy and the wave effects must be included in the model in order to predict the corresponding holdup and pressure gradient in real systems. The case study

of Fig. 2 will be used as a reference to study the wave effect on the holdup and pressure gradient in Section 3 (Fig. 11b).

The MTF closure relations for turbulent flows are tested by comparison of the predicted holdup and pressure drop with the experimental data of Espedal (1998) that correspond to air–water flow in the smooth stratified flow regime. The data was obtained in $D = 0.0601$ m rough wall (equivalent sand roughness, $\kappa_s = 0.006$ mm) slightly downward inclined pipe ($\beta = 0.104°$, 0.5°, 1° and 3°). The associated gas and liquid Reynolds numbers correspond to turbulent flow in both phases. Therefore, the MTF model was applied with the rough wall friction factors expressions (see Appendix A). The comparison shown in Fig. 3 substantiates the validity of the MTF closure relations for stratified turbulent flows. The comparisons shown in Fig. 3 include also the experimental data corresponding to small interfacial waves. Compared to the smooth interface data, the comparison with the small wave data of pressure gradient is somewhat less favorable; indicating that some augmentation of the shear stresses is already required. However, it appears that in this case the discrepancies do not justify the introduction of empirical corrections for the wave effect.

In general, gas–liquid systems represent an extreme case of $\rho_2/\rho_1 \to 0$ and $\mu_2/\mu_1 \to 0$, where typically, the interaction between the phases is one-way, in particular in co-current flow in horizontal and upward inclined pipes. The momentum transfer is from the fast gas phase to the slower liquid phase. In the MTF closure relations these gas–liquid systems are associated with $U_1/U_2(\varepsilon/(1-\varepsilon))^2/X^2 \ll 1$, whereby $F_2 \to 1$ and $F_{i2} \to 1$.

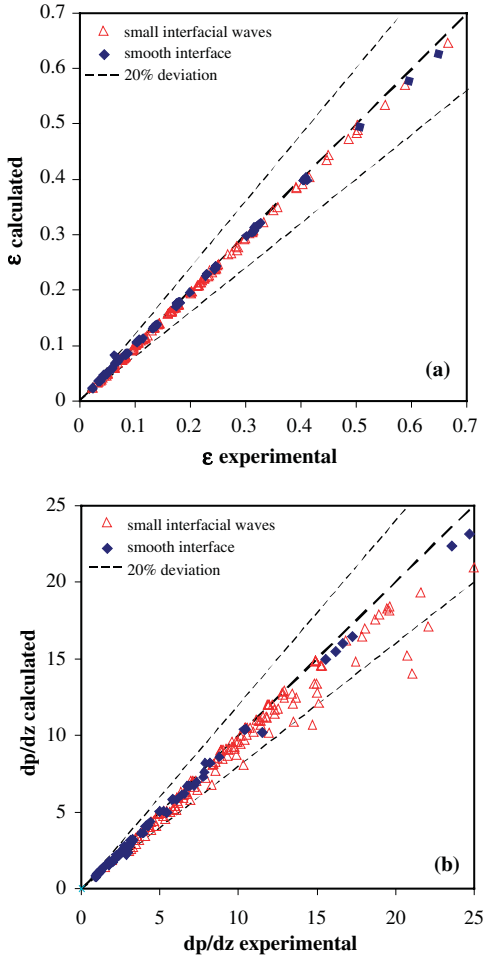

Fig. 3. The MTF model predictions depicted versus experimental data of Espedal (1998) for gas–liquid stratified flow in a downward inclined 0.0601 m diameter pipe. Data correspond to smooth interface or to small interfacial waves: (a) holdup and (b) dimensionless frictional pressure gradient.

Accordingly, the interfacial shear is dominated by the flow of the gas phase, and the gas wall shear stress is well represented by the single-phase-based closure relation.

Two-fluid closure relations are challenged by cases of stratified flow of fluids of similar viscosities and densities, whereby similar velocities of the two-phases are encountered. In such cases the interaction between the flows of the two phases is two-way. In the MTF closure relations, values of $X^2(1-\varepsilon)^2/\varepsilon^2 \approx O\{1\}$ are obtained for similar flow rates (and holdups) of the two fluids, whereby both $F_1 \neq 1$ and $F_2 \neq 1$. Consequently, the interaction factors affect the values of the wall shear stresses of both the upper and lower phases. Also, depending on the flow rates ratio and holdups, the interfacial shear can be dominated by either the lower phase or the upper phase (see Eq. (8.1)). Therefore, it is of particular interest to test the closure relations in the extreme case of pseudo-single-phase laminar or turbulent flows with $\tilde{\rho} = \rho_1/\rho_2 = 1$ and $\tilde{\mu} = \mu_1/\mu_2 = 1$.

The case of horizontal laminar flow with $\tilde{\mu} = 1$ corresponds to Poiseuille flow at the mixture flow rate of $U_m = (U_{1s} + U_{2s})$, even for $\rho_1 \neq \rho_2$. The results of TF models can then be compared with the exact solution for the pressure drop and holdup variations with the flow rates ratio, $q = Q_1/Q_2$ (e.g. Ullmann et al., 2004). In case of single-phase turbulent flows, power-law models for the velocity profiles ($\tilde{u} \propto \tilde{y}^{1/m}$) and the corresponding power-law relation for the wall friction factor (Schlichting, 1979) can be used to represent an 'exact' solution for the pressure drop. For instance, for the 1/7 power-law velocity profile, the wall friction factor is given by $f = 0.079/Re_m^{0.25}$, while for the 1/9 power-law $f = 0.046/Re_m^{0.2}$, where $Re_m = \rho D U_m/\mu$. The 'exact' holdups vs. flow rates ratio associated with the power-law velocity profiles were obtained by numerical integration of the velocity profile over the flow area of each of the phases.

The deviations of MTF model predictions from the 'exact' solutions in case of laminar flow ($n_{1,2} = 1$) and for turbulent flow (e.g. $n_{1,2} = 0.2$) are shown in Figs. 4 and 5 respectively. These figures show the ratio between the MTF model predictions and the corresponding 'exact' results obtained for the fluids flow rates ratio (Figs. 4 and 5a) and for the pressure gradient (Figs. 4 and 5b) vs. the lower layer thickness, h/D. The deviation of the predicted flow rates ratio is less than 1% in the range of $0.1 < q < 10$ (for extreme q ratios it is less than ≈5% for turbulent flow and less than 10% for laminar flow). The maximal deviations of the pressure gradient are less than 2%. For comparison, the predictions obtained by the conventional TF closure relations, which ignore the F-interaction factors (e.g. Ullmann et al., 2003a), are also shown in these figures. The application of the conventional TF model requires adjustment of the hydraulic diameter according to the relative velocity of the phases. For $h/D < 0.5$, the upper phase is the faster. Thus, in the TF model $f_i = f_2$ is assumed and the hydraulic diameters are calculated considering the interface as 'stationary' with respect to the upper phase and as 'free' with respect to the lower phase. Vice versa, for $h/D > 0.5$, $f_i = f_1$ and the interface is considered as 'stationary' with respect to the faster lower phase and as 'free' with respect to the upper phase. Evidently, the deviations of the TF model from the 'exact' values of the pressure drop and flow rates ratio are much larger than those of the MTF model. These figures also demonstrate the difficulties encountered in applying the TF model for this apparently simple case. In the vicinity of $h/D = 0.5$, $q = 1$, a solution (which is consistent with these assumptions) can be obtained only if the interface is considered as 'free' with respect to both phases in the calculation of the hydraulic diameters. While this assumption significantly improves the TF model predictions in the vicinity of $q \simeq 1$, the prediction of the pressure gradient deteriorates for $q \neq 1$. A criterion must then be adopted for switching between the solutions obtained with these two alternative models ('stationary' or 'free' interface). Such a switching, however, introduces discontinuity in the TF model predictions, which is avoided by the MTF closure relations. The MTF closure relations suggest a smooth transition between upper phase dominated flow with $h/D < 0.5$, to lower phase dominated flow when $h/D > 0.5$. As already discussed with reference to Fig. 2, the weaknesses of the TF model become even more crucial in inclined flows, where a different body force is driving the two layers and backflow situations are encountered (see also in Ullmann et al., 2003b).

Espedal (1998) reported also 59 holdup measurements for free interface single phase water flow in a downward inclined pipe, $\beta = 0.104°$, 0.5°, 1° and 3° ($D = 0.0601$ m and equivalent sand roughness, $\kappa_s = 0.006$ mm). All the data correspond to turbulent flow. This is an interesting test case for the MTF closure relations. Evidently, in free surface liquid flow $\tau_i \approx 0$ is expected, implying that the interfacial shear is still dominated by the gas phase, albeit $U_L \gg U_G \equiv 0$ (and thus $U_2/U_1 = 0$). In the commonly used two-fluid models, $\tau_i = 0$ must be imposed. However, in the MTF model, $\tau_i = 0$ evolves from the closure relations for the interfacial shear (Eqs. (8)). Although $U_L \gg U_G \equiv 0$ for $U_{2s} \equiv U_{Gs} = 0$, the condition for the second form of Eq. (8.1) is satisfied,

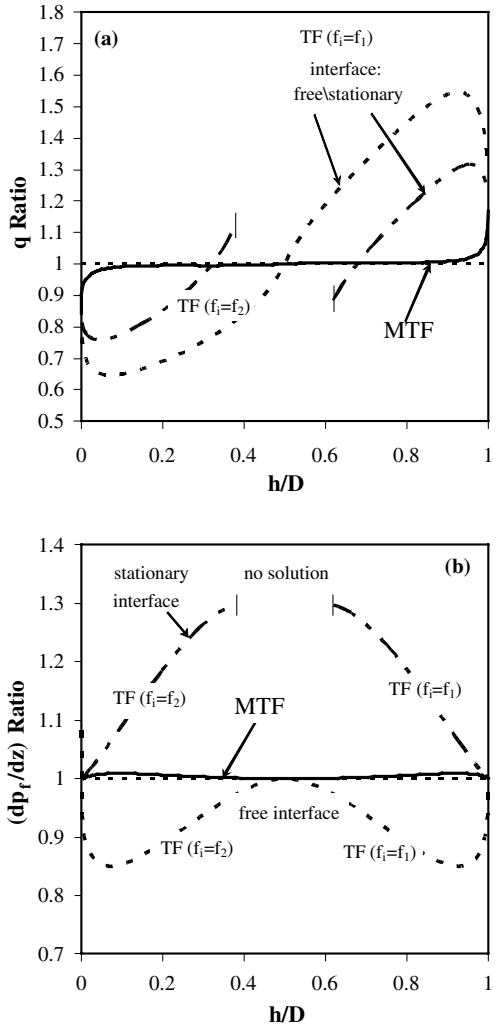

Fig. 4. Validation of the MTF model predictions for the case of pseudo-single-phase laminar horizontal flow, $\tilde{\mu} = 1$ and comparison with the TF model predictions. The predictions are normalized by those corresponding to the exact solution of Posiulle flow: (a) flow rates ratio and (b) frictional pressure gradient ratio (dashed line: 'free interface' assumed in the hydraulic diameter calculation of both phases).

suggesting that the interfacial shear should be calculated based on the (zero) flow of the gas phase, whereby $\tau_i = 0$ is obtained.

Fig. 6 shows the predicted vs. experimental values of the holdup for the free surface liquid flow. The favorable agreement substantiates the closure relation used for the wall shear stress. In particular, it is worth noting that although the friction factor f_L ($= f_1$) is calculated based on hydraulic diameter that considers the interface as 'stationary', the F_1-interaction factor introduces the necessary correction and correctly represent the situation of a 'free' liquid interface.

3. Wavy stratified flow

3.1. The interface curvature

In wavy stratified flows, the interface curvature is dominated by the secondary flows, which develop in both phases. Measurements of holdup (ε) and wetted perimeter (ϕ_0) in gas–liquid systems indicate extended wall

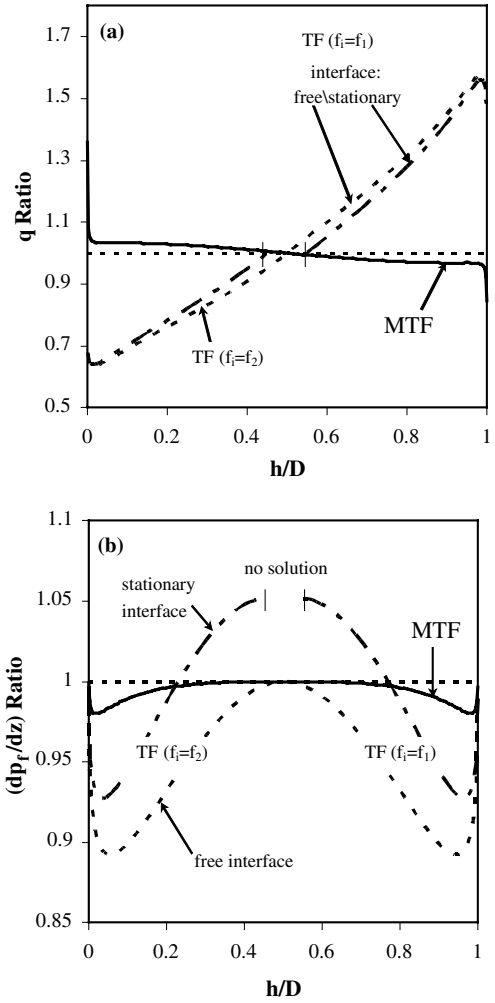

Fig. 5. Validation of the MTF model predictions for the case of pseudo-single-phase turbulent flow, $\tilde{\mu} = 1$, $\tilde{\rho} = 1$, and comparison with the TF model predictions. The predictions are normalized by those corresponding to the 'exact' single phase power-law model solution ($n_{1,2} = 0.2$ corresponding to 1/9 power-law velocity profile): (a) flow rates ratio and (b) frictional pressure gradient ratio (dashed line: 'free interface' assumed in the hydraulic diameter calculation of both phases).

wetting even in gravity dominated systems corresponding to large Eo_D (e.g. Hart et al., 1989; Chen et al., 1997; Ottens, 1998). This implies a concave rather than plane interface. Possible mechanisms suggested in the literature include: dragging of the liquid by gas secondary flows (e.g. Laurinat et al., 1985; Lin et al., 1985) and/or pumping action due to lateral pressure gradient induced by the waves (Fukano and Ousaks, 1989).

The evolution of secondary flows in gas–liquid wavy stratified flow is attributed to the non-uniformity of the interfacial roughness experienced by the flow of the turbulent gas-phase; the wall roughness is smaller than the apparent roughness of the wavy interface. These secondary flows have been studied experimentally (e.g. Suzanne, 1985; Strand, 1993; Lopez, 1994; Flores et al., 1995) and numerically (Magnaudet, 1989; Jayanti et al., 1990; Liné et al., 1996; Nordsveen and Bertelsen, 1997; Meknassi et al., 2000). It is worth noting that in most of these numerical studies the gas–liquid interface was considered to be plane, while in wavy stratified pipe flow the liquid interface was observed to be a concave. An additional closure relation is thus required for the modeling to account for the variation in the interface shape.

Hamersma and Hart (1987) and Hart et al. (1989) suggested a constant liquid film thickness, δ to model the stratified flow configuration. The following experimental correlation was obtained for the measured wetted wall fraction, Θ, in terms of the liquid holdup and the liquid Froude number, Fr_L:

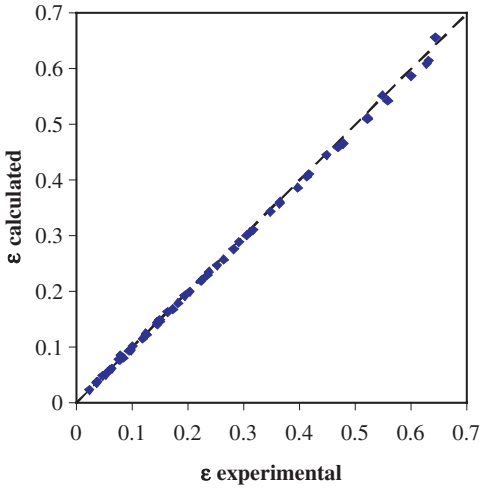

Fig. 6. Comparison of the MTF holdup predictions with experimental data of Espedal (1998) for free interface liquid flow in a downward inclined 0.0601 m diameter pipe.

$$\Theta = \frac{\tilde{S}_L}{\pi} = \frac{\phi_0}{\pi} = 0.52\varepsilon^{0.374} + 0.26Fr_L^{0.58}; \quad Fr_L = \frac{\rho_L U_L^2}{(\rho_L - \rho_G)gD}; \quad \varepsilon = 4\Theta\frac{\delta}{D} \tag{11}$$

This correlation was obtained for low liquid load and high gas flow rates where the constant film thickness approximation may reasonably describe the flow configuration. A more appropriate approximation for the interface shape is a constant curvature arc (see Table 1). This geometry was used by Chen et al. (1997) combined with the correlation of Hart et al. (1989) as a closure for ϕ_0 (in Chen et al., 1997, $\phi_0 \equiv \theta$ and $\pi - \phi^* \equiv \theta_i$). However, the use of correlation (11) combined with the momentum equations to determine ϕ^* (hence, the interface shape) is not strictly physical, as the curvature does not evolves from the axial momentum equations. The momentum equations should be used to determine ϕ_0 (or the holdup). For instance, in gravity dominated systems and in the absence of secondary flows the interface is plane ($\phi^* = \pi$) and the momentum equations yield the solution for ϕ_0 and the corresponding holdup. In this case the solution is not necessarily compatible with correlation (11). As a matter of fact, ϕ^* (which is directly related to the interface shape) is determined by lateral curving forces, for which a closure relation is required.

The value of ϕ^* can be deduced from simultaneous measurements of the holdup and the wetted perimeter, $\tilde{S}_L \equiv \tilde{S}_1 = \phi_0$ (see Table 1). The following implicit equation has to be then solved for the unknown curvature, ϕ^*

$$\varepsilon_{exp} - \frac{1}{\pi}\left\{\phi_0^{exp} - \frac{1}{2}\sin(2\phi_0^{exp}) - \frac{\sin^2\phi_0^{exp}}{\sin^2\phi^*}\left[\phi^* - \pi - \frac{1}{2}\sin(2\phi^*)\right]\right\} = 0 \tag{12}$$

Data of simultaneous measurements of ϕ_0 and ε were reported by Chen et al. (1997) and Ottens (1998). These data correspond to gravity-dominated systems of large Eo_D, where surface tension effects are negligible, and therefore, the interface in the stratified smooth regime is practically plane, $\phi^* = \pi$. In the stratified wavy regime, the secondary flows are of the order of the shear velocity, $u^* = \sqrt{\tau_G/\rho_G}$. Hence, the curvature deviations from a plane interface are assumed here to be correlated with the ratio of the gas phase shear stress, $\tau_G \equiv \tau_2$ (representing the momentum of the secondary flow) acting against the gravity restoring force, $(\rho_L - \rho_G)g\cos\beta D$. The data however indicate additional dependence of the curvature on the liquid layer velocity and on the interface length. Based on the experimental data of Chen et al. (1997) and Ottens (1998), the following correlation has been obtained for ϕ^*:

$$\phi^* = \pi + 2tg^{-1}\left\{57.2\left|\frac{\tau_G}{(\rho_L - \rho_G)g\cos\beta D}\right|^{0.5}\left|\frac{U_L}{U_G}\right|^{0.5}\tilde{S}_i\right\} \tag{13}$$

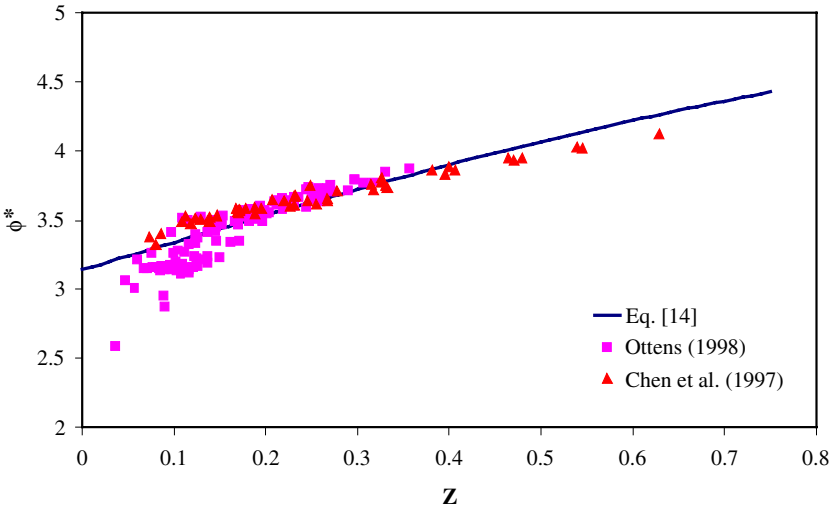

Fig. 7. Experimental correlation for the interface curvature in wavy stratified gas–liquid flow (Eq. (13)): comparison with values implied by the data of Chen et al. (1997) and Ottens (1998) ($Z = 57.2|(U_L\tau_G\tilde{S}_i^2)/(U_G(\rho_L - \rho_G)g\cos\beta D)|^{0.5}$).

The values predicted for ϕ^* by this correlation are compared with the experimental data in Fig. 7. The rms of the correlation is 0.008 and it reasonably describes the variation of the interface curvature in both data sets. This correlation suggests that the approach toward the annular configuration ($\phi_0 \to \pi$, $\phi^* \to 2\pi$) is enhanced by increasing the shear of the gas phase, reducing the gravity force and increasing the liquid to gas velocity ratio.

It is worth emphasizing that the wall shear stress in the gas phase is generally well-predicted by the closure relation used in the stratified smooth regime (e.g. Kowalski, 1987; Liné and Fabre, 1996; Espedal, 1998). Thus, given the holdup and the phases flow rates, the corresponding value of ϕ^* can be conveniently obtained by Eq. (13) (using Eq. (4) for $\tau_G \equiv \tau_2$), independently of the wave effects on the interfacial shear and the liquid wall shear.

3.2. Augmentation of the interfacial shear and liquid wall shear

The interfacial waves are known to have a pronounce effect on the interfacial shear and on the liquid wall shear stress. Assuming the wall shear stress in the gas phase ($\tau_G \equiv \tau_2$) is unaffected by the interfacial waves, experimental data of simultaneous measurements of the holdup and pressure drop, combined with Eq. (13) for the interface curvature ϕ^*, can be used to deduce the corresponding values of the 'experimental' liquid wall shear stress, $\tau_1 \equiv (\tau_L)_{exp}$, and interfacial shear, $(\tau_i)_{exp}$, using the following procedure. When the flow rates and ε^{exp} are given, the two implicit Eqs. (12) and (13) are first solved to determine the two unknowns ϕ_0 and ϕ^*. In cases measurements of ϕ_0 are also available (e.g. Chen et al. (1997) and Ottens (1998) data), the experimental value of ϕ_0 and the corresponding solution of Eq. (12) for ϕ^* are used. Once the flow geometry has been determined, the two momentum balances, Eqs. (1.1) and (1.2) can be solved for the two unknowns $(\tau_L)_{exp}$, $(\tau_i)_{exp}$.

To this aim, the data-base shown in Table 2 was used. The data correspond to the region of large amplitude 2-D and 3-D waves. The gas phase is turbulent, while the liquid phase is either laminar or turbulent, depending on its viscosity and flow rate. The transitional liquid Reynolds number was taken as $Re_L \equiv Re_1 = 1000$. Note however, that the Reynolds number is defined based on $D_1 = 4A_1/(S_1 + S_i)$ (see Eqs. (5)), whereas the data correspond to $U_L/U_G \ll 1$, where the effective hydraulic diameter of the liquid phase is $D_1^{eff} = 4A_1/S_1$. Therefore, the corresponding effective transitional Re_L is about 2000.

The so-obtained $(\tau_i)_{exp}$ and $(\tau_L)_{exp}$ were compared with the corresponding values predicted by the closure relations of smooth stratified flow (Eq. (8) and (3)). The ratios between the 'experimental' values and those predicted for smooth interface were used to derive correlations for the empirical correction factors to the friction factors $f_1 \equiv f_L$ and f_i that account for the wave augmentation effects.

Table 2
Data-base for holdup and pressure drop in wavy stratified flow

Source	Fluids	Liquid properties			D [mm]	Inclination	Number of tests	Pressure [bar]
		ρ_L [kg/m^3]	μ_L [kg/(ms)]	σ [N/m]	κ_s [mm]			
Chen et al. (1997)	Air/kerosene	813	~0.0018	0.029	77.9 0	Horizontal	48	1.9–2.4
Espedal (1998)	Air/water	998	~0.001	~0.06	60.1 0.006	0.104–3° down 0.104–0.5° up	192	1
Ottens (1998)	Air/water	998	~0.001	~0.06	51 0	Horizontal 0–1° down 0–2° up	112	1
Badie et al. (2000)	Air/water Air/oil	1000 865	~0.001 0.040	0.037 0.032	78 0	Horizontal	39 30	1

The wave effect on the interfacial shear has been correlated by

$$F_{iw} = \frac{\tau_i}{(\tau_i)_{smooth}} - 1 = 10.25\left(\frac{\rho_G}{\rho_{G0}}\right)^{0.33} Fr_{Gs}^{0.65}\varepsilon^{0.33} + 0.1Ca^{1.2} - 15\beta_I \tag{14.1}$$

$$Fr_{Gs} = \left[\frac{\rho_G}{(\rho_L - \rho_G)Dg\cos\beta}\right]^{0.5}|U_{Gs}|; \quad Ca = \frac{|U_G - U_L|\mu_L}{\sigma} \tag{14.2}$$

where ρ_{G0} represents the air density at atmospheric pressure ($=1.2$ kg/m^3), β_I is the inclination (in radians, positive for co-current down-flow, negative for concurrent upflow). Note however that the data used to derive the correlation correspond to horizontal or slightly inclined pipes, with mild effect of the β_I term. If application of Eq. (14) is considered for steeper (downward) inclinations, this term should be better discarded.

The ratio of the wave effect on the interfacial shear and wall shear has been correlated by

$$F_W = \frac{\tau_i/(\tau_i)_{smooth}}{\tau_L/(\tau_L)_{smooth}} = 5.15Fr_{Ls}^{0.75}\varepsilon^{-0.6} + 0.25Ca^{0.7} \tag{15.1}$$

where

$$Fr_{Ls} = \left[\frac{\rho_L}{(\rho_L - \rho_G)Dg\cos\beta}\right]^{0.5}|U_{Ls}| \tag{15.2}$$

Accordingly, in wavy stratified flow the closure relation for the interfacial shear (second form of Eq. (8.1) is augmented by the factor $(1 + F_{iw})$. The closure relation for the liquid wall shear (Eq. (3)) is augmented by the factor $F_{LW} = (1 + F_{iw})/F_W$, in case the liquid wall shear stress is not reversed due to backflow ($F_L \equiv F_1 \geqslant 0$). Otherwise, for $F_L < 0$ and $F_{LW} > 1$, $F_{LW} = 1$ is assumed (backflow is not augmented due to wave effects).

The fit between these two correlations and the values implied by the experimental data points are shown in Fig. 8. The rms of correlation (14.1) and (15.1) are $\simeq$0.05 and 0.03, respectively. The scatter on the resulting wall shear augmentation factor, F_{LW} (Fig. 8c) is however larger. The exceptional large deviations, where the correlation under predicts the values implied by the data (Ottens, 1998; Espedal, 1998) correspond to up-flow with low gas velocities, close to the transition to slug flow and the triple solution region (see discussion below, Fig. 11). The few highly scattered points of Badie et al. (2000) correspond to extremely low liquid flow rates and holdups ($\varepsilon < 0.01$), and their deviation may be a result of limited measurement accuracy.

The correlations and the data indicate that large waves can amplify the interfacial shear and the liquid wall shear up to ten times the value predicted for smooth stratified flow (Fig. 8a and c). The wave effect on the liquid wall shear is not restricted to thin liquid layers. The largest wave augmentation effect is indicated by the data corresponding to high liquid viscosity. It is worth noting that the correlation for F_{iw} is highly influenced by the oil–air flow data, and more data corresponding to viscous liquids as well as for high pressure systems (high ρ_G) are needed to substantiate the experimental correlations for F_{iw}.

The data of $(F_{iw})_{exp} = (\tau_i)_{exp}/(\tau_i)_{smooth} - 1$ was compared also with the widely used correlation of Andritsos and Hanratty (1987). Following their assumption of a plane interface, one obtains a large scatter in $(F_{iw})_{exp}$

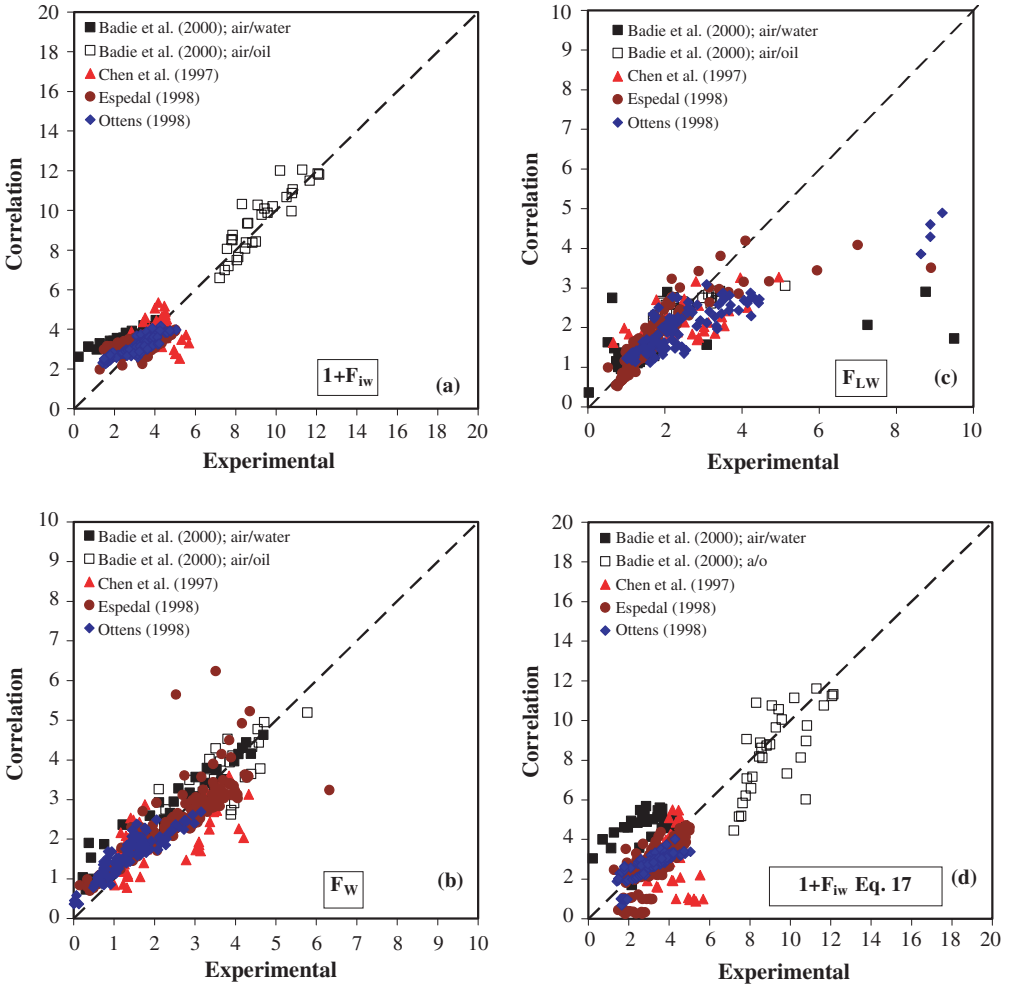

Fig. 8. Values of the wave augmentation factors obtained by the experimental correlations in comparison with the values implied by the data-base of Table 2: (a) interfacial shear augmentation, (b) ratio of interfacial shear and wall shear augmentation, (c) wall-shear augmentation and (d) modified Andritsos and Hanratty (1987) correlation for the interfacial shear augmentation.

(deduced from the data-base of Table 2) compared to their original correlation. However, adopting the structure of their correlation for the curved interface geometry (using Eq. (13) for ϕ^*), the following equation was fitted to the $(F_{iw})_{exp}$ values

$$F_{iw} = 37.2\tilde{h}_{hav}^{0.9}\left(\frac{U_{Gs}}{U_{Gs,t}} - 1\right); \quad \tilde{h}_{hav} = \frac{\pi\varepsilon}{4\tilde{S}_L}; \quad U_{Gs,t} = 5\left(\frac{1.2}{\rho_G}\right)\ [\mathrm{m/s}] \tag{16}$$

The $U_{Gs,t}$ is the critical gas superficial velocity for transition from stratified smooth to stratified wavy (SS/SW) suggested by Andritsos and Hanratty (1987). The results of this fit are shown in Fig. 8d. Compared to Fig. 8a the scatter in Fig. 8d is larger. Moreover, negative values of F_{iw} result from Eq. (16) due to miss-prediction of the critical gas-velocity for the SS/SW transition, should be discarded. Therefore, the correlation given in Eq. (14.1) appears to be preferable.

It is worth noting that a flow pattern map or a criterion for transition to the stratified wavy regime (e.g. Taitel and Dukler, 1976; Brauner and Moalem Maron, 1993) is still needed as a complementary information also for Eqs. (14) and (15). This information is required in order to identify the range of operational conditions for which the wave effects should be considered.

3.3. Comparison with experimental data

Predicted versus experimental values of liquid holdup and axial pressure gradient corresponding to the data-base of Table 2 are shown in Figs. 9 and 10. Considering the variety of gas–liquid systems studied, the predictions are satisfactory. The deviations in most cases are less than 20% for both the predicted holdup and the predicted pressure drop. Exceptional are the holdup data of Chen et al. (1997) for relatively thick liquid layers (corresponding to low gas superficial velocities), which tend to be somewhat systematically over-predicted. These data imply higher wave augmentation of the interfacial shear than that offered by correlation (14). More pronounced deviations are obtained for some of the holdup data of Ottens (1998). However, in contrast to the comparison with the data of Chen et al. (1997), in this case the discrepancies are inconsistent and characterize a limited number of specified data points. The four noticeably under predicted holdups correspond to 1° upflow, while the four over predicted points correspond to 2° upflow. Both cases are for the lowest gas flow rates where stratified flow was experimentally obtained, close to the transition to slug flow. The reasons for these deviations deserve further elaboration.

Fig. 11a shows the variation of the holdup with increasing the air flow rate at a constant water flow rate in a 2° upward inclined pipe. As shown, a good agreement with the relevant data is obtained at relatively high air flow rates. The large discrepancies between the predictions and the data appear at lower air flow rates, where the holdup is very sensitive to small variations in the air flow rate. A small reduction of the experimental air

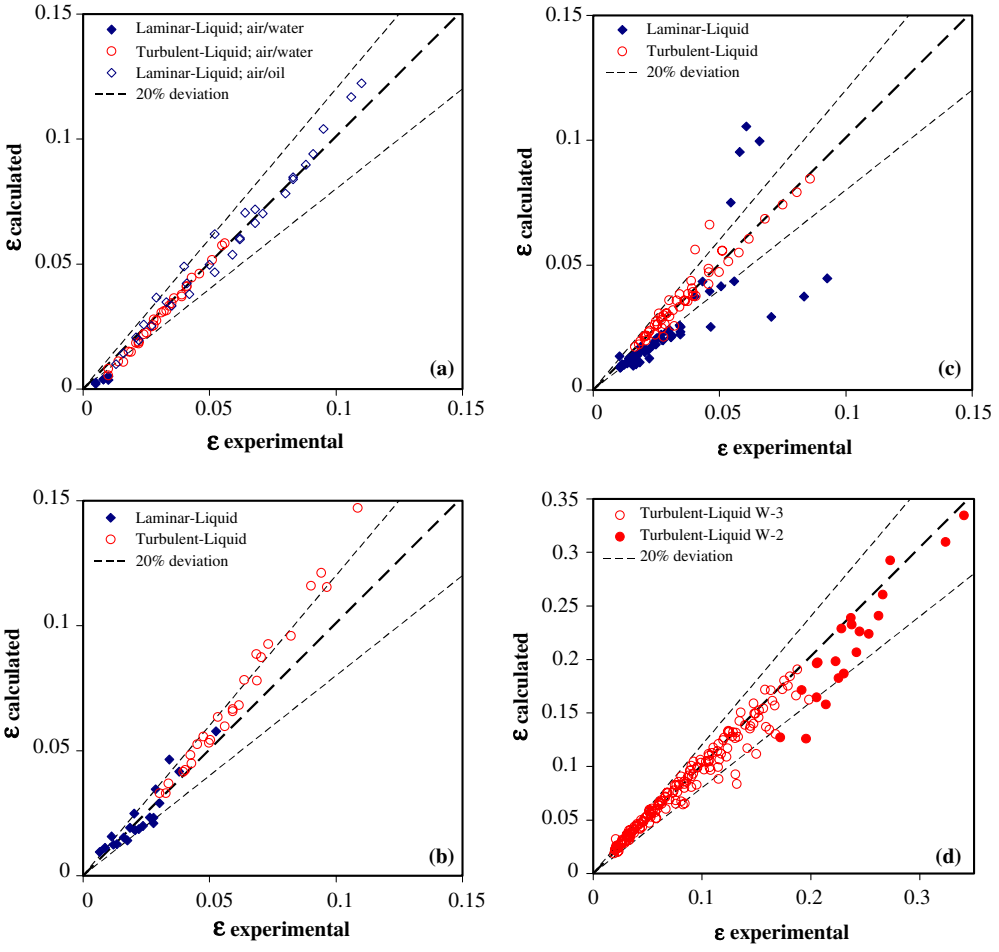

Fig. 9. Comparison of the MTF model predictions for the holdup with data obtained in horizontal, upward and downward inclined flows in the large wave stratified flow regime: (a) Badie et al. (2000), (b) Chen et al. (1997), (c) Ottens (1998) and (d) Espedal (1998).

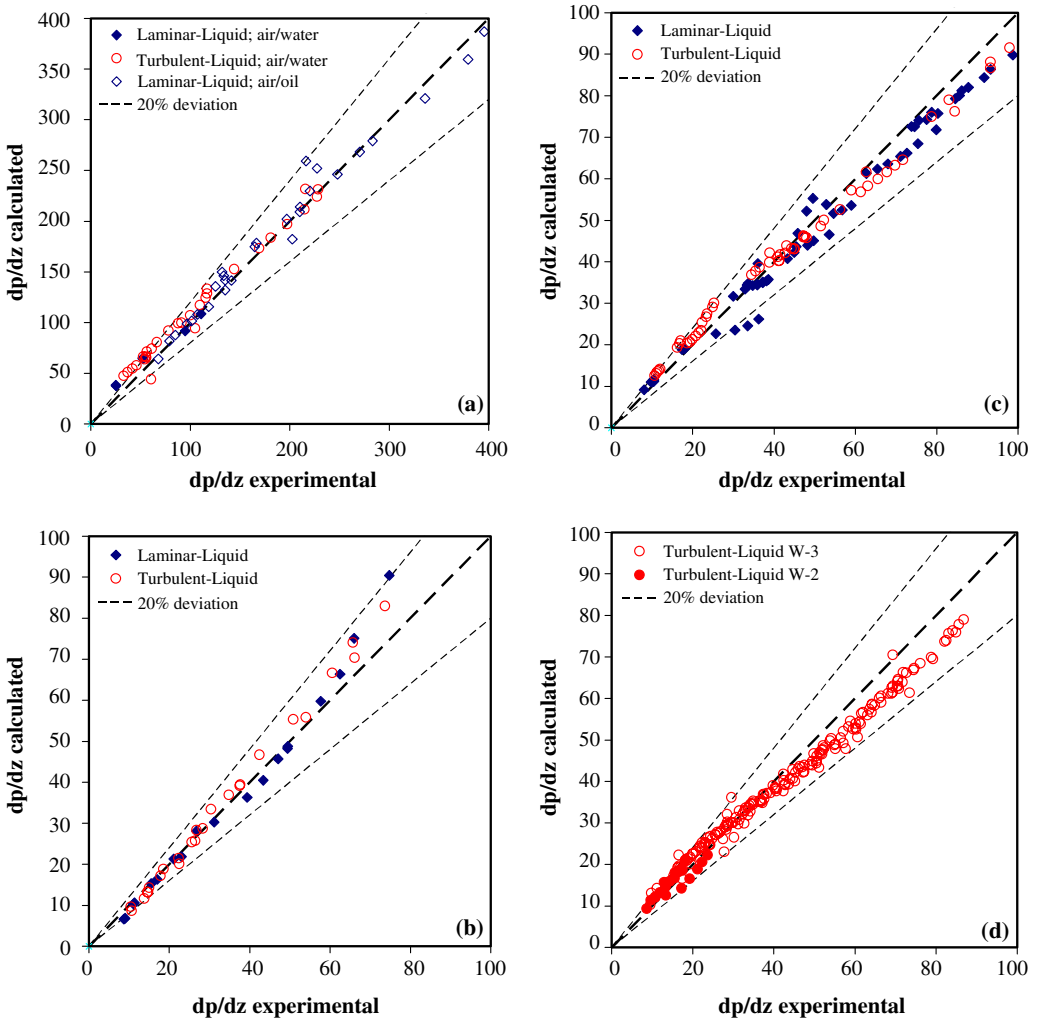

Fig. 10. Comparison of the MTF model predictions for the pressure gradient with data obtained in horizontal, upward and downward inclined flows in the large wave stratified flow regime: (a) Badie et al. (2000), (b) Chen et al. (1997), (c) Ottens (1998) and (d) Espedal (1998).

flow rate would cause a dramatic increase of the water holdup. For these high holdups, the stratified flow configuration become unstable due to wave bridging phenomena and slug flow is usually observed. This region of air and water flow rates is close to the triple solution region discussed with reference to Fig. 2 (see also Ullmann et al., 2003b). Depicting the predicted holdup at a constant air flow rate in the vicinity of the triple solution region (Fig. 11b) reveals additional sources for miss prediction of the data.

Fig. 11b was obtained for the same operational conditions as those of Fig. 2. The results are obviously different here, due to the inclusion of the wave effects on the interfacial curvature and the augmentation of the wall and interfacial shear stresses (F_{Lw} and F_{iw}). Similarly to Fig. 2, the triple solution region corresponds to relatively low U_{Ls}, with turbulent air and laminar water flows (L_L–T_G). However, compared to Fig. 2, the triple solution region extends here to a wider range of liquid flow rates, mainly as a result of the interfacial shear stress augmentation. In the triple solution region, reversed wall shear ($F_L \equiv F_l \leqslant 0$) due to backflow (BF) is encountered for the high holdup and intermediate holdup solutions. Therefore, according to discussion in Section 3.2, $F_{Lw} = 1$ is assumed for these two holdups. Augmentation of the wall shear stress is included only for the calculation of the lowest holdup in the triple solution region, as well as for sufficiently high U_{Ls}, where $F_L > 0$ indicates no backflow also for the relatively high holdups (in the single solution region).

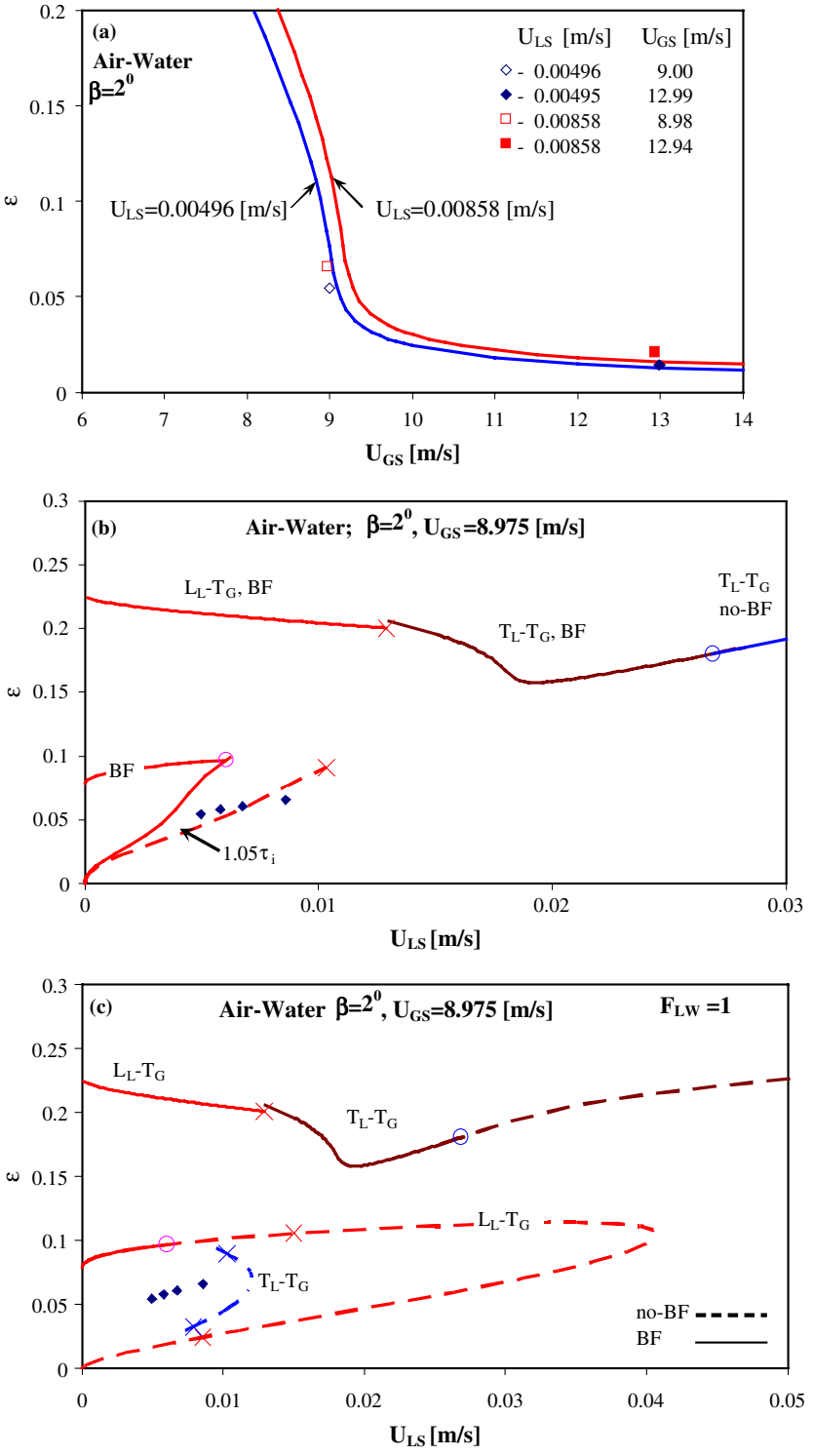

Fig. 11. Multiple solutions for gas–liquid wavy stratified flow in a 2° upward inclined pipe ($D = 5.1$ cm) and sensitivity of the predictions to small variation in the model parameters: (a) variation of the holdup with increasing air flow rate at a constant water flow rate, (b) variation of the holdup at a constant air flow rate in the vicinity of the triple solution region and (c) same as (b) however with $F_{LW} = 1$. Symbols: (×) laminar–turbulent transition; (○) $\tau_L = 0$, transition from backflow (BF) to no-BF point; (♦) experimental (Ottens, 1998).

Four experimental points that are available for the conditions of Fig. 11b are depicted in the figure. They are located close to the predicted triple solution region, however, they are over predicted by the model. As demonstrated in the figure, in this particular case, the model predictions are dramatically improved with a minor (5%) increase of the interfacial shear. This sensitivity is obviously beyond the accuracy that can be expected from the general correlation for F_{iw}, which has been obtained based on data for horizontal, downward and upward inclined flows.

The model prediction in the triple solution region is also sensitive to the wall-shear augmentation. To demonstrate this sensitivity, the results obtained with $F_{Lw} = 1$ (also with no backflow, dashed line) are shown in Fig. 11c. In this case, the predicted triple solution range extends to even higher liquid flow rates. However, for these higher flow rates, the flow is turbulent in the liquid layer. Therefore, the solution for T_L–T_G is also depicted in Fig. 11c. The proximity of the experimental data to the various optional results of the model indicates the sensitivity of predictions to small variations in either the wave augmentation factors of the shear stresses, or the in the laminar/turbulent transitional Reynolds number. Therefore, any prediction in this region should be approached with extra care, and one should examine all possible solutions and their sensitivity to the model empirical correction factors and assumptions.

Finally, to demonstrate the generality of experimental correlations for the stratified wavy regime, the predictions of the MTF model are tested against pressure drop and holdup data obtained for different physical properties and tube diameters than those included in the data-base of Table 2. Fig. 12 shows comparisons with data of Hoogendoorn (1959) for horizontal air–oil flow in large diameter tube ($D = 14$ cm) corresponding to the stratified wavy regime. The MTF model predictions for the experimental flow rates are aligned along the correlation obtained by Hoogendoorn (1959) for this data. Moreover, the constant C of that correlation was reported to slightly increase with the tube diameter (the corresponding data were not shown in Hoogendoorn, 1959), which appears to be consistent with the diameter effect indicated by the MTF closure relations (Fig. 12b). Favorable agreement is also indicated by the comparison with the holdup data corresponding

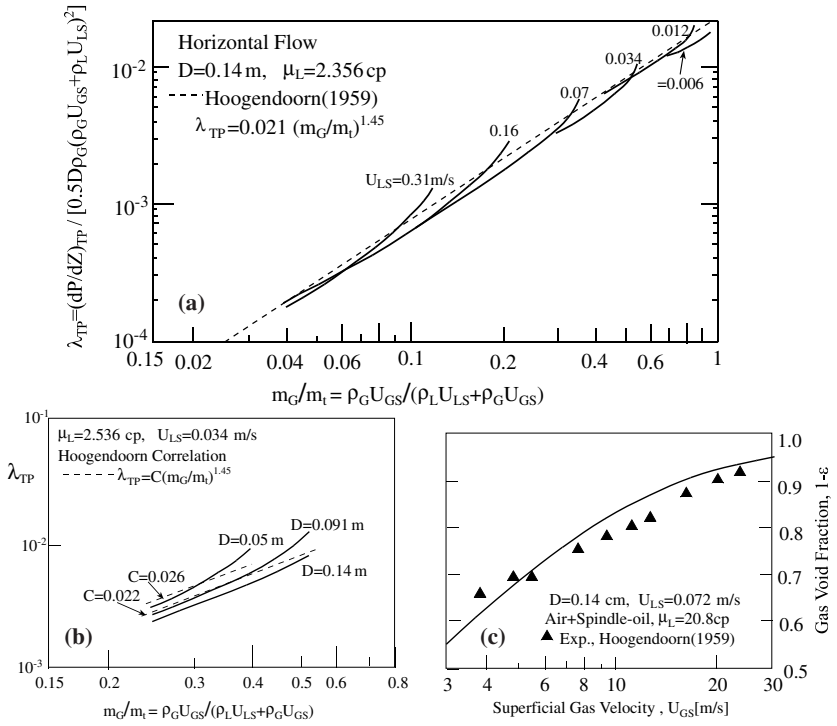

Fig. 12. Validation of the MTF model predictions in the wavy stratified flow regime against experimental data of Hoogendoorn (1959) for oil–air horizontal wavy stratified flow: (a) Hoogendoorn two-phase friction factor, (b) effect of tube diameter on the two-phase friction factor and (c) holdup for air/spindle–oil flow. The coordinates used are those of Hoogendoorn (1959).

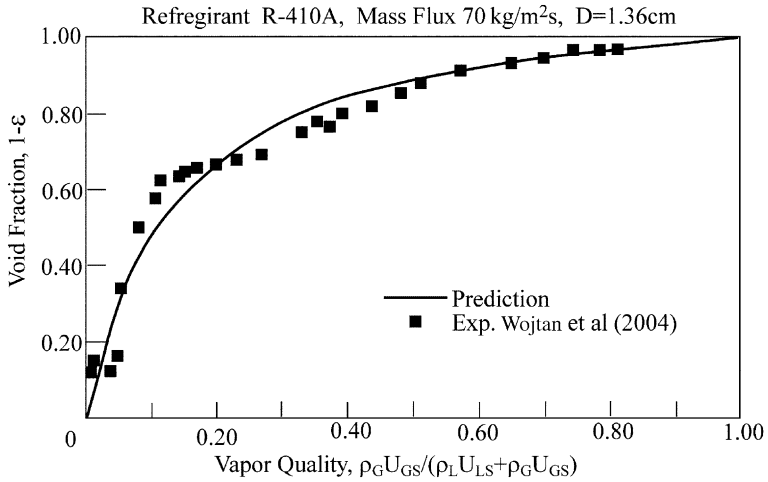

Fig. 13. Validation of the MTF model predictions against experimental data of Wojtan et al. (2004) for vapor–liquid refrigerant (410A) wavy stratified flow in $D = 1.36$ cm tube.

to wavy stratified flow of air/spindle-oil (Fig. 12c). Similarly, a good agreement is indicted by the comparison of the MTF model predictions with the holdup data reported by Wojtan et al. (2004) for vapor–liquid refrigerant flows (Fig. 13). These data correspond to small diameter tube ($D = 1.36$ cm), high density of the gas phase (35 times that of atmospheric air) and small liquid viscosity (15% of water). To summarize, the favorable comparisons with a wider range of system parameters further substantiate the validity of the MTF closure relations.

4. Conclusions

Accurate prediction of the holdup and pressure drop in stratified flow via 1-D two-fluid models require reliable closure relations for the wall and interfacial shear stresses and for the interface shape.

In gravity dominated systems and in the smooth stratified flow regime, the interface is practically flat. Still, the commonly used closure relations for the wall and interfacial shear stresses that are borrowed from single-phase flow theory and/or correlations may yield poor predictions of the pressure drop and holdup due to the negligence of the effects of the interaction between the two phases flowing in the same channel.

The theory-based closure relations for laminar stratified flow, recently derived in Ullmann et al. (2004) for the wall and interfacial shear stresses, were extended to make them applicable also for cases of turbulent flow in either or both of the phases. The new closure relations are formulated in terms of the commonly used single-phase-based expressions, which are augmented by the two-phase interaction factors. In particular, the expressions obtained for the wall shear are capable of representing the change in the direction of the wall shear-stress when gravity driven backflow of either of the phases is encountered in the near wall region (i.e. in the heavy phase in concurrent up-flow, or in the light phase in concurrent down-flow).

The TF model predictions obtained with these new closure relations (MTF model) were validated by comparison with the results obtained for the case of pseudo-single-phase turbulent pipe flow and with pressure drop and holdup data of Espedal (1998) for turbulent gas–liquid stratified flow with a smooth interface. These closure relations are basically valid for gas–liquid and liquid–liquid gravity dominated systems in the stratified smooth regime. However, they were further used as a platform for introducing necessary empirical corrections to represent the wave effects in the gas–liquid stratified wavy regime.

Based on the experimental data of Ottens (1998) and Chen et al. (1997) for holdups and wall wetted perimeters in the stratified wavy regime, a new correlation was obtained for the curvature of the gas–liquid interface. According to this correlation, the time-averaged shape of the wavy gas–liquid interface is concave. The annular configuration is gradually approached by increasing the shear of the gas phase or the liquid to gas velocity ratio, and is enhanced by reducing the gravity force.

The correlation for the interfacial curvature was combined with pressure drop and holdup data from the literature for concurrent horizontal, upward and downward inclined stratified flows, to obtain new empirical corrections for the wave effect on the interfacial shear stress and on the liquid wall shear stress. The correlations and the data indicate that the large waves can increase the interfacial shear and the liquid wall shear by up to ten times the value predicted for smooth stratified flow.

The results of this study indicate that the new closure relations are essentially representing correctly the interaction between the phases over a wide range of the stratified flow parameters space in the stratified smooth and stratified wavy regime. However, miss prediction of the holdup may be encountered in gas–liquid up-flow, under (or close to) conditions where multiple solutions are obtained, due to the high sensitivity of the results to small variation in the interfacial and liquid wall shear stresses. The prediction in these regions should be approached with extra care, and one should examine all possible solutions and their sensitivity to the model empirical correction factors and assumptions.

Appendix A. Rough wall surface

The Blasius type power-law model for the wall friction factor (Eq. (5.1)) is valid for hydrodynamic-smooth wall. In case of turbulent flow in rough pipes, the wall friction factors are calculated based on Haland (1983) equation. For single phase turbulent flow this equation yields

$$\frac{1}{\sqrt{f_{1s,2s}}} = -3.6\log_{10}\left(\frac{6.9}{Re_{1s,2s}} + \left(\frac{\kappa_s}{3.7D}\right)^{1.11}\right) \tag{A.1}$$

where κ_s is the wall roughness. This equation is a good explicit approximation to the Colebrook (1939) implicit equation (with 1.5% precision for $4\times10^4 \leqslant Re \leqslant 10^8$, $0 \leqslant \tilde{\kappa}_s = \kappa_s/D \leqslant 5\times10^{-2}$). Thus, in case of turbulent flow of either of the phases, the wall friction factor f_1 or f_2 (used in Eqs. (3) and (4), respectively) are given by

$$\frac{1}{\sqrt{f_{1,2}}} = -3.6\log_{10}\left(\frac{6.9}{Re_{1,2}} + \left(\frac{\kappa_s}{3.7D_{1,2}}\right)^{1.11}\right); \quad Re_{1,2} = \frac{\rho_1|U_{1,2}|D_{1,2}}{\mu_{1,2}}; \quad D_{1,2} = \frac{4A_{1,2}}{(S_{1,2}+S_i)} \tag{A.2}$$

The corresponding Martinelli parameter in case of turbulent flow in both phases is then given by

$$X^2 = \frac{f_{1s}}{f_{2s}}\frac{\rho_1}{\rho_2}|q|q \tag{A.3}$$

The interfacial friction factors f_{i1}, f_{i2} are calculated by Eq. (A.2) with $\kappa_s = 0$. The effective power-law exponents for particular Reynolds numbers $Re_{1,2}$ (needed in Eqs. (3), (4) and (6)) are evaluated by

$$n_1 = \frac{\log(f_1^+/f_1^-)}{\log(Re_1^+/Re_1^-)}; \qquad n_2 = \frac{\log(f_2^+/f_2^-)}{\log(Re_2^+/Re_2^-)} \tag{A.4}$$

where $f_{1,2}^+$, $f_{1,2}^-$ are the wall friction factors obtained by Eq. (A.2) for $Re_{1,2}^+ = (1+\delta_{Re})Re_{1,2}$ and $Re_{1,2}^- = (1-\delta_{Re})Re_{1,2}$, respectively (e.g. $\delta_{Re} = 0.01$).

Note that in cases of smooth pipe wall, Eqs. (A.1)–(A.4) with $\kappa_s = 0$ can replace the power-law expressions (Eq. (5.1)) for the friction factors.

References

Andreussi, P., Persen, L.N., 1987. Stratified gas–liquid flow in downwardly inclined pipes. Int. J. Multiphase Flow 13, 565–575.

Andritsos, N., Hanratty, T.J., 1987. Influence of interfacial waves in stratified gas–liquid flows. AIChE J. 33, 444–454.

Badie, S., Hale, C.P., Lawrence, C.J., Hewitt, G.F., 2000. Pressure gradient and holdup in horizontal two-phase gas–liquid flows with low liquid loadings. Int. J. Multiphase Flow 26, 1525–1543.

Brauner, N., Moalem Maron, D., 1989. Two-phase liquid–liquid stratified flow. Physico-Chem. Hydrodynam. 11, 487–506.

Brauner, N., Moalem Maron, D., 1993. The role of interfacial shear modeling in predicting the stability of stratified two-phase flow stability. Chem. Eng. Sci. 48, 2867–2879.

Brauner, N., Rovinsky, J., Moalem Maron, D., 1996. Determination of the interface curvature in stratified two-phase systems by energy considerations. Int. J. Multiphase Flow 22, 1167–1185.

Brauner, N., Rovinsky, J., Moalem Maron, D., 1998. A two-fluid model for stratified flows with curved interfaces. Int. J. Multiphase Flow 24, 975–1004.
Chen, X.T., Cai, X.D., Brill, J.P., 1997. Gas–liquid stratified-wavy flow in horizontal pipelines. J. Energy Resour. Technol. 119, 209–216.
Cohen, L.S., Hanratty, T.J., 1968. Effect of waves at a gas–liquid interface on a turbulent air flow. J. Fluid Mech. 31, 467–479.
Colebrook, C.F., 1939. Turbulent flow in pipes with particular reference to the transition region between the smooth and rough pipe laws. J. Inst. Civil Eng. 11, 133–156.
Espedal, M., 1998. Experimental investigation of stratified two-phase pipe flow in small inclinations. Ph.D. Thesis, Department of Applied Mechanics, NTNU, Trondheim, Norway.
Flores, A.G., Crowe, K.E., Griffith, P., 1995. Gas-phase secondary flow in horizontal, stratified and annular two-phase flow. Int. J. Multiphase Flow 21, 207–221.
Fukano, T., Ousaks, A., 1989. Prediction of the circumferential distribution of film thickness in horizontal and near horizontal gas–liquid annular flow. Int. J. Multiphase Flow 15, 403–419.
Gorelik, D., Brauner, N., 1999. The interface configuration in two-phase stratified flow, Int. J. Multiphase Flow 25, 877–1007.
Hagiwara, Y., Esmaeilzadeh, E., Tsutsui, H., Suzuki, K., 1989. Simultaneous measurements of liquid film thickness, wall shear stress and gas flow turbulence of horizontal wavy two-phase flow. Int. J. Multiphase Flow 15, 421–431.
Haland, S.E., 1983. Simple and explicit formulas for the friction factor in turbulent pipe flow. J. Fluids Eng. 105, 89–90.
Hart, J., Hamersma, P.J., Fortuin, J.M.H., 1989. Correlations predicting frictional pressure drop and liquid holdup during horizontal gas–liquid pipe flow with a small liquid holdup. Int. J. Multiphase Flow 15, 947–964.
Hamersma, P.J., Hart, J., 1987. A pressure drop correlation for gas–liquid pipe flow with a small liquid holdup. Chem. Eng. Sci. 42, 1187–1196.
Hoogendoorn, C.J., 1959. Gas–liquid flow in horizontal pipes. Chem. Eng. Sci. 9, 205–217.
Jayanti, S., Wilke, N.S., Clarke, D.S., Hewitt, G.F., 1990. The prediction of turbulent flows over roughened surfaces and its application to interpretation of mechanisms of horizontal annular flow. Proc. R. Soc. Lond. 431, 71–88.
Kawaji, M., Anoda, Y., Nakamura, H., Tasaka, T., 1987. Phase and velocity distributions and holdup in high-pressure steam/water stratified flow in a large diameter horizontal pipe. Int. J. Multiphase Flow 13, 145–159.
Kowalski, J.E., 1987. Wall and interfacial shear stress in stratified flow in a horizontal pipe. AIChE J. 33, 274–281.
Laurinat, J.E., Hanratty, T.J., Jepson, W.P., 1985. Film thickness distribution for gas–liquid annular flow in horizontal pipe. Physico-Chem. Hydrodynam. 6, 179–195.
Lin, T.J., Jones, O.C., Lahey, R.T., Block, R.C., Muase, M., 1985. Film thickness measurements and modeling in horizontal annular flows. Physico-Chem. Hydrodynam. 6, 197–206.
Liné, A., Fabre, J., 1996. Stratified flow. In: International Encyclopedia of Heat and Mass Transfer. Innodata Corporation, pp. 1015–1021.
Liné, A., Masbernat, L., Soualmia, A., 1996. Interfacial interaction and secondary flows in stratified two-phase flow. Chem. Eng. Commun. 141–142, 303–329.
Lopez, D., 1994. Ecoulements diphasiques à phases séparées à faible contenu de liquide. Thèse de doctorat, INP Toulouse, France.
Magnaudet, J., 1989. Interactions interfaciales en écoulement à phases séparées. Thèse de doctorat, INP Toulouse, France.
Meknassi, F., Benkirane, R., Liné, A., Masbernat, L., 2000. Numerical modeling of wavy stratified two-phase flow in pipes. Chem. Eng. Sci. 55, 4681–4697.
Nordsveen, M., Bertelsen, A.F., 1997. Wave induced secondary motions in stratified duct flow. Int. J. Multiphase Flow 23, 503–522.
Oliemans, R.V.A., 1987. Modelling of gas-condensate flow in horizontal and inclined pipes. In: Pipeline Engineering Symposium—ETCE, Presented at ASME, Dallas, Texas.
Ottens, M., 1998. Gas–liquid flow through pipes and T-junctions. Ph.D. thesis, University of Amsterdam, ISBN 90-5651-055-X.
Ottens, M., Kinkspoor, K., Hoefsloot, H.C.J., Hamersma, P.J., 1997. A new type of video imaging technique for measuring interfacial waves in stratified-wavy gas/liquid pipe flow. In: Proceedings of the 4th World Conference on Heat Transfer, Fluid Mechanics and Thermodynamics, Brussels, Belgium, 2–6 June, p. 1190.
Ottens, M., Kinkspoor, K., Hoefsloot, H.C.J., Hamersma, P.J., 1999. Wave characteristics during co-current gas–liquid flow pipe flow. Exp. Thermal Fluid Sci. 19, 140–150.
Schlichting, H., 1979. Boundary Law Theory. McGraw-Hill series in Mechanical Engineering.
Strand, O., 1993. An experimental investigation of stratified two-phase flow in horizontal pipes. Ph.D. Thesis, University of Oslo, Norway.
Suzanne, C., 1985. Structure de l'écoulements stratifié de gaz et de l'INPT, Toulouse, France.
Taitel, Y., Dukler, A.E., 1976. A model for predicting flow regime transitions in horizontal and near horizontal gas–liquid flow. AIChE J. 22, 47–55.
Ullmann, A., Brauner, N., 2004. Closure relations for the shear stresses in two-fluid models for core-annular flows. Multiphase Sci. Technol. 16, 355–387.
Ullmann, A., Zamir, M., Ludmer, Z., Brauner, N., 2003a. Stratified laminar counter-current flow of two liquid phases in inclined tube. Int. J. Multiphase Flow 29, 1583–1604.
Ullmann, A., Zamir, M., Gat, S., Brauner, N., 2003b. Multi-holdups in co-current stratified flow in inclined tubes. Int. J. Multiphase Flow 29, 1565–1581.
Ullmann, A., Goldstien, A., Zamir, M., Brauner, N., 2004. Closure relations for the shear stresses in two-fluid models for stratified laminar flows. Int. J. Multiphase Flow 30, 877–900.
Vlachos, N.W., Paras, S.V., Karabelas, A.J., 1997. Liquid-to-wall shear stress distribution in stratified/atomization flow. Int. J. Multiphase Flow 23, 845–863.

Vlachos, N.A., Paras, S.A., Karabelas, A.J., 1999. prediction of holdup, axial pressure gradient and wall shear stress in wavy stratified and stratified/atomization gas/liquid flow. Int. J. Multiphase Flow 25, 365–376.

Watterson, J.K., Cooper, R.K., Spedding, P.L., 2002. Prediction of pressure loss and holdup in two-phase horizontal stratified roll-wave pipe flow. Ind. Eng. Chem. Res. 41, 6621–6622.

Wojtan, L., Ursenbacher, T., Thome, J.R., 2004. Interfacial measurements in stratified types flow. Part 2: Measurements for R22 and R-410A. Int. J. Multiphase Flow 30, 125–137.